Iran. J. Biotechnol. October 2021;19(4): e2575 DOI: 10.30498/ijb.2021.201202.2575

Research Article

Recombinant Expression, Purification and Characterization of Pyridoxal 5′-phosphate Synthase from *Geobacillus* sp. H6a, Thermophilic Bacterium Producing Extracellular Vitamin B6

Adulwit Sinthusiri, Chamaiporn Champasri, Yanee Trongpanich*

Department of Biochemistry, Faculty of Science, Khon Kaen University, Khon Kaen, 40002, Thailand

*Corresponding author: Yanee Trongpanich, Department of Biochemistry, Faculty of Science, Khon Kaen University, Khon Kaen, 40002, Thailand; Tel: +66-868607899; Fax: +66-43342911; E-mail: yantro@kku.ac.th

Background: Pyridoxal 5′ -phosphate synthase (PLPS) is present in deoxyxylose 5′-phosphate-independent of the *de novo* vitamin B6 biosynthesis pathway. This enzyme complex consists of PdxS and PdxT, which function as synthase and glutamine amidotranferase respectively to produce PLP.
Objectives: This study aimed to clone, express, and purify PLPS of *Geobacillus* sp. H6a, followed by its characterization.
Material and Methods: The *PdxS* and *PdxT* genes were amplified from *Geobacillus* (*Gh*) sp. H6a. Recombinant vectors pET28a-GhpdxS and pET28a-GhpdxT were constructed and the resulting His-tagged proteins were expressed in *E. coli* BL21(DE3). The soluble rGhpdxS and rGhpdxT were purified via nickel-affinity chromatography and cation-exchange chromatography. The mixture of rGhpdxS and rGhpdxT was further characterized.
Results: The molecular weights of rGhpdxS and rGhpdxT were estimated to be 35 and 23 kDa by SDS-PAGE, respectively. The native form of rGhpdxS showed hexamer and dodecamer, whereas those of rGhpdxT were a monomer upon detection with non-denaturing gel electrophoresis and gel filtration. A molar ratio of 1:1 of rGhpdxS:rGhpdxT showed the highest PLP synthesis activity (4.16 $U.mg^{-1}$) and was used for analyzing the biochemical properties. The kinetic values were obtained by using glyceraldehyde 3-phosphate, ribose 5-phosphate, and glutamine as the substrates. The rGhPLPS showed pentose phosphate isomerization without triose phosphate isomerase activity. The metal ions affected PLP synthesis activity. The optimum pH and optimum temperature of rGhPLPS were 9 and 70 °C, respectively. The rGhPLPS was active over a broad range of temperatures and pH values.
Conclusions: These results support the potential of rGhPLPS as a candidate for industrial application.

Keywords: Geobacillus, Pyridoxal 5′-phosphate synthase**,** Recombinant Proteins, Thermophilic bacterium

1. Background

Pyridoxal 5′ -phosphate (PLP) is the biocatalytically active form of vitamin B6, which refers to the pyrimidine vitamer derivatives: pyridoxine (PN), pyridoxal (PL), pyridoxamine (PM) and their respective 5′-phosphate esters: pyridoxine 5′ -phosphate (PNP), pyridoxal 5′ -phosphate (PLP), pyridoxamine 5′ phosphate (PMP) (1).

PLP functions as a coenzyme for more than 140 enzymatic reactions in all living organisms. It belongs to five of the six enzyme classes related to the amino acid, glucose, and lipid metabolisms (oxidoreductases EC 1, transferases EC 2, hydrolases EC 3, lyases EC 4, isomerases EC 5) (1). In humans, PLP deficiency has been associated with several pathologies including cancer and diabetes. The studies in *Drosophila* suggest that PLP deficiency accompanied by hyperglycemia can lead to DNA damage and may contribute to cancerogenesis (2).

To date, all forms of vitamin B6 have been manufactured by a chemical process. The biotechnological synthesis of vitamin B6 is attractive, as it reduces waste and also provides further economic benefits (3). Biosynthetic processes for vitamin B6 are divided into two distinct

Copyright *© 2021 The Author(s); Published by National Institute of Genetic Engineering and Biotechnology. This is an open access article, distributed under the terms of the Creative Commons Attribution-NonCommercial 4.0 International License (http://creativecommons.org/licenses /by-nc/4.0/) which permits others to copy and redistribute material just in noncommercial usages, provided the original work is properly cited.*

pathways: salvage and *de novo* pathway. The salvage pathway is not a direct synthesis of new vitamin B6. Each form of vitamin B6 is interconvertible by the action of four enzymes. PLP, PMP, and PNP are dephosphorylated by the alkaline phosphatase (EC 3.1.3.1) or PL phosphatase (EC 3.1.3.74). PL, PM and PN are rephosphorylated by PL kinase (EC 2.7.1.3511), while PMP and PNP are converted to PLP in a reaction catalyzed by PN (PM) oxidase (EC 1.4.3.5) (4). This pathway is found in almost all living organisms.

The *de novo* biosynthesis pathway synthesizes new vitamin B6 from phosphate sugars and amino acids. There are two different *de novo* biosynthesis pathways: one uses deoxyxylose 5′-phosphate (DXP) as a precursor whilst the second does not. The first *de novo* biosynthesis pathway is a DXP dependent, which is found in *Escherichia coli* and a small group of proteobacteria.

In this pathway, 4-phosphohydroxy-L-threonine and DXP were used as substrates to form PNP by the PdxJ (EC 2.6.99.2) and PdxA (EC 1.1.1.262) (1, 5).

The second *de novo* biosynthesis pathway is a DXP independent or ribose 5-phosphate (R5P)-dependent pathway, which is widely found in bacteria, archaea, fungi, Plasmodia, and plants (5). This *de novo* biosynthesis pathway consumes R5P or ribulose 5-phosphate (Ru5P), in combination with either glyceraldehyde 3-phosphate (G3P) or dihydroxyacetone phosphate (DHAP) and glutamine as substrates. The DXP independent pathway synthesizes PLP through the PLP synthase (PLPS) complex (5, 6).

The intact PLPS complex comprises 12 PdxS and 12 PdxT subunits. PdxS and PdxT have distinct and spatially separated catalytic functions (6). The PdxT or glutaminase subunit is a glutamine amidotransferase, which is in class I (Triad family), using a Cys-His-Glu catalytic triad to produce ammonia by hydrolysis of glutamine. PdxS is a synthase subunit that catalyzes not only PLP formation, but also the isomerization of R5P to Ru5P, and DHAP to G3P (7).

PLPS appears to be potentially useful in pharmacology due to its absence in humans (6), and it is the key step of the biosynthesis pathway of vitamin B6 in other pathogenic organisms such as Plasmodia (8). The construction of PLPS in bacterial strains for vitamin B6 production has also been reported, suggesting opportunities for industrial bioproducts (5). Many *PdxS* and *PdxT* genes have been cloned, expressed, and characterized in *Escherichia coli* from biological sources, including *Bacillus subtilis* (9, 10), *Geobacillus stearothermophilus* (6), *Streptococcus pneumoniae* (11), *Mycobacterium tuberculosis* (12), *Thermotoga maritima* (13) , *Pyrococcus horikoshii* (14), *Saccharomyces cerevisae* (7, 15, 16), Plasmodia (8, 17, 18), *Arabidopsis thaliana* and *Ginkgo biloba* (19). In our previous study, thermophilic bacterium *Geobacillus* sp. H6a (Gh), collected from a hot spring in the North of Thailand, produces extracellular vitamin B6 in PMP and PM forms (20). The expression analysis of *GhpdxS* and *GhpdxT* genes encoded GhpdxS and GhpdxT proteins to form PLPS from *Geobacillus* sp. H6a had studied. The results show that the pathway of vitamin B6 biosynthesis from *Geobacillus* sp. H6a possesses a DXP independent pathway which constituted *GhpdxS* and *GhpdxT* genes. Phylogenetic analysis of deduced amino acids is similar to Pdx1/SNZ and Pdx2/SNO family, respectively (21).

2. Objectives

Given that *Geobacillus* sp. H6a could produce vitamin B6 outside the cell and PLPS is the key step of the biosynthesis pathway of vitamin B6. To gain more information on PLPS from *Geobacillus* sp. H6a, this study shows the purification and characterization of rGhPLPS.

3. Materials and Methods

3.1. Materials

A Genomic DNA mini kit, High-Speed Plasmid Mini Kit, and a Gel/PCR DNA fragment extraction kit were purchased from Geneaid Biotech Ltd. (Taipei, Taiwan). A *Taq* DNA Polymerase was purchased from RBC Bioscience (Taipei, Taiwan). A Ni Sepharose 6 Fast Flow column, Superdex 200, Superdex 75, and Vivaspin® 20 were from GE Healthcare Bio-Science AB (Sweden). All other chemicals were analytical grade.

3.2. Cloning of Ghpdx genes in E. coli BL21(DE3)

The *GhpdxS* and *GhpdxT* genes were separately cloned in pET28a (+) vector and expressed in *E. coli* BL21 (DE3). The genomic DNA of *Geobacillus* sp.H6a was isolated by a Genomic DNA mini kit.

The *GhpdxS* gene (accession number FJ 497249) and *GhpdxT* gene (accession number FJ 497250)

were amplified by touchdown PCR and the specific primers were designed to incorporate *Nhe*I and *Bam*HI restriction sites **(Table 1)**.

The touchdown PCR condition consisted of 3 cycles of denaturation at 95 °C for 1 min and annealing at 62 °C for 1 min, 4 cycles of 60 °C for 1 min, 23 cycles of 58 °C for 1 min and final extension at 72 °C for 2 min. The pET28a (+) vector was isolated using a High-Speed Plasmid Mini Kit and subsequently digested with the same restriction enzymes. The resulting PCR products digested with the restriction enzymes and the digested pET28a (+) vector were purified by using a Gel/PCR DNA fragment extraction kit. The resulted constructs entitled pET28a-GhpdxS and pET28a-GhpdxT were transformed into *E. coli* BL21(DE3) by using the heat shock method. Colony PCR was used to check the transformants. DNA sequencing was carried out by First Base Laboratories (Malaysia).

3.3. Expression Optimization of Recombinant GhpdxS (rGhpdxS) and Recombinant GhpdxT (rGhpdxT)

A single colony of *E. coli* BL21(DE3), harboring pET28a-GhpdxS or pET28a-GhpdxT was grown in LB medium containing 50 $\mu g.mL^{-1}$ kanamycin, until an optical density (OD600) reached 0.5. The expressions of rGhpdxS and rGhpdxT were induced and optimized by adding different concentrations of isopropyl-1-thio-D-galactopyranoside (IPTG), different incubation temperatures (25 °C, 30 °C, 37 °C), and times (0, 1, 3, 6 h). Cell pellets were harvested and resuspended with buffer A (50 mM Tris-HCl, 10% glycerol, 10 mM NaCl, pH 8.0) containing 1 mM phenylmethylsulfonyl fluoride (PMSF). The cells were lysed by using ultrasonication and the resulting cell lysate was centrifuged at 10,000´g for 15 min at 4 °C. The protein was observed on 12% separating gel of SDS-PAGE electrophoresis. Protein concentration was determined by Bradford assay and the absorbance was monitored at 595 nm with bovine serum albumin as a standard protein (22).

3.4. Purification of Recombinant GhpdxT

The supernatant obtained from lysed *E. coli* BL21(DE3) cells harboring pET28a-GhpdxT was loaded on Ni Sepharose 6 Fast Flow column after equilibration with buffer B (50 mM Tris-HCl, 10% glycerol, 0.5 M NaCl, pH 8.0) containing 10 mM imidazole. The non-specific binding proteins were washed with buffer B containing 20 mM imidazole at the flow rate of 0.25 mL.min-1 and the fractions were collected at 1.0 mL/fraction. The rGhpdxT was eluted with buffer B containing 100 mM imidazole. The active fractions were pooled, concentrated, and desalted by Vivaspin® 20. The recombinant enzyme was kept in buffer A and was stored at 4 °C for further characterization.

3.5. Purification of Recombinant GhpdxS

For purification of recombinant GhpdxS with Ni Sepharose 6 Fast Flow column, condition and buffers were used with the same as described for rGhpdxT. The rGhpdxS was purified further by DEAE-cellulose, the anion-exchanged column (Sigma, USA) (1×10 cm). The column was equilibrated and washed with 50 mM Tris-HCl, 10% glycerol, 0.2 M NaCl, pH 8.0 at a flow rate of 1.0 $mL.min^{-1}$, and each fraction was collected at 5.0 mL. The bound enzyme was eluted with the linear gradient of 0.2 - 0.4 M NaCl in the same buffer. The active fractions were pooled, concentrated, and desalted by Vivaspin® 20.

The rGhpdxS was kept in buffer A and was stored at 4 °C for further characterization.

3.6. Gel Filtration Chromatography

The Superdex 200 column (1×85 cm) was equilibrated and eluted with 50 mM Tris-HCl, 0.15 M NaCl,

Table 1. The oligonucleotide sequences of specific primers. The underlines showed the recognition sites of the restriction enzymes.

Name	Sequence
FpdxSNhe	5′- ATTGCTAGCATGGCATTGACAGGTACGGACC-3′
RpdxSBam	5′- TTTTGGATCCTTACCAGCCGCGTTCTTGCATC-3′
5PdxTNhe	5′- AAAGCTAGCATGAAAATAGGTGTACTTGGACTGC-3′
3PdxTBam	5′- TTGGGATCCTTACTTGAGGCTTGACGCC-3′

10% glycerol pH 8.0 at flow rate of 0.25 mL.min^{-1}. Fractions were collected at 1 mL/fraction and measured absorbance at 280 nm. The gel filtration standards (Bio-Rad) composes of thyroglobulin (670 kDa), g-globulin (158 kDa), ovalbumin (44 kDa), myoglobin (17 kDa), and Vitamin B12 (1.35 kDa) were also loaded on the column and were used for determination of the molecular weight of rGhpdxS. Gel filtration on Superdex 75 column (1×80 cm) was used to determine the molecular weight of rGhpdxT. Condition and buffer used with the same as that of rGhpdxS.

3.7. The rGhpdxT Activity Assay

The rGhpdxT was assayed in two steps, according to Wrenger *et al* (18), by measuring the formation of glutamate, which is subsequently converted to 2-oxoglutarate by glutamic dehydrogenase with NADP+ as a co-substrate. The reaction mixture (0.3 mL) consisted of 10 mM glutamine and enzyme in 50 mM Tris-HCl, pH 8.0. The reaction mixture was incubated at 30 °C for 10 min, and the reaction was stopped by boiling for 1 min. To measure the amount of glutamate formed, 0.3 mL of the sample was incubated in 1 mL of 50 mM Tris-HCl, pH 8.0 containing 1 mM EDTA, 500 µM NADP+, and 7 units of Glutamic Dehydrogenase from bovine liver (Sigma Chemical Co., USA). The reaction mixture was incubated at 30 °C for 90 min. Finally, the samples were centrifuged at 14,000×g for 1 min, and the absorbance was determined at 340 nm. The activity was calculated with the molar extinction coefficient of 6220 M-1 cm^{-1} of NADPH. One unit of the enzyme was defined as the amount of the enzyme required to produce 1 nmol of NADPH per min.

3.8 The rGhpdxS Activity Assay

The rGhpdxS was assayed by measuring the increasing absorbance at 414 nm corresponding to the production of PLP (23). The reaction mixture (0.2 mL) consisted of 1 mM R5P, 1 mM G3P, 10 mM ammonium chloride and enzyme in a 50 mM Tris-HCl pH 8.0. The reaction mixture was incubated at 37 °C for 30 min, after which the fine particles were removed by centrifugation. One unit of the enzyme was defined as the amount of the enzyme required to produce 1 nmoL of PLP per min.

3.9. PLPS Activity Assay

The rGhPLPS was assayed by modification of the method of Wada and Snell (24). The produced PLP reacts with phenylhydrazine to form a colored hydrazone, measured by the increasing absorbance at 405 nm. The reaction mixture (0.2 mL) consisted of 1 mM R5P, 1 mM G3P, 5 mM glutamine, rGhpdxS and rGhpdxT in a 50 mM Tris-HCl pH 9.0. The reaction mixture was incubated at 70 °C for 30 min. The reaction was stopped by adding trichloroacetic acid (TCA) at a final concentration of 8% and centrifuged at 10,000 g for 1 min to remove proteins. The 2% phenylhydrazine reagent (dissolved in 10 N sulfuric acid) was added to a final concentration of 0.1% and left at room temperature for 10 min. One unit of the enzyme was defined as the amount of the enzyme required to produce 1 nmoL of PLP per min.

The kinetic parameters of rGhPLPS were determined using G3P, R5P (0.02 – 1.5 mM), and glutamine (1 – 20 mM) in three independent trials at 70 °C. Approximately 0.1 mg of rGhPLPS consisting of 0.05 mg rGhpdxS and 0.05 mg rGhpdxT, was used in each assay. The *Km* and *Vmax* values were calculated by using GraphPad Prism software version 6.01 (GraphPad Software, Inc.).

3.10. Effect of pH and Temperature on PLPS Activity

The effects of pH on rGhPLPS activity were determined in 50 mM buffers of: glycine-HCl (pH 3.0), sodium acetate (pH 4.0 - 5.0), sodium phosphate (pH 6.0), HEPES (pH 7.0 - 8.0), Tris-HCl (pH 9.0), glycine-NaOH (pH 10.0). The pH stability was investigated after pre-incubation of enzyme in different pH buffers for 60 min at 25 °C, followed by measuring the residual activity using the standard assay as previously described.

The effects of temperatures on rGhPLPS activity were determined in 50 mM Tris-HCl (pH 9.0) at temperatures from 25 °C to 80 °C. Thermal stability was measured after preincubation of enzyme in 50 mM Tris–HCl buffer (pH 9.0) for 60 min at various temperatures (between 25 °C to 80 °C), followed by measuring residual activity using the standard assay as described above.

3.11. Effects of Metal Ions on PLPS Activity

The effects of metal ions were performed by adding various metal salts, KCl, NaCl, $MnSO_4$, $CoCl_2$, $CuSO_4$, $CaCl_2$, $NiSO_4$, $MgCl_2$, $ZnCl_2$, $FeSO_4$, and $FeCl_3$, at the concentration range of 0.5 – 10 mM. The rGhPLPS

activity of the enzyme in the absence of metal ions was defined as 100% activity.

3.12. Effect of Substrate Specificity on PLPS Activity

Enzyme substrate specificity was determined by measuring activity against 1 mM R5P, Ru5P, dihydroxyacetone phosphate, and DL-glyceraldehyde 3-phosphate in 50 mM Tris–HCl buffer (pH 9.0). The standard enzyme assays were then performed. The reaction products of PLP were identified by using UV-VIS spectrophotometer Microplate reader (EZ read 2000, Biochrome) and the reversed-phase isocratic HPLC described by Argoudelis (25).

4. Results

4.1. Cloning and Expression of Ghpdx Genes

The *GhpdxS* and *GhpdxT* genes from *Geobacillus* sp. H6a genomic DNA was amplified **(Fig. 1)** and separately cloned in to the pET28a (+) vector. Both the resulting plasmids were designated as pET28a-GhpdxS and pET28a-GhpdxT and the DNA sequences were verified to ensure that no unintended mutations had occurred. The theoretical molecular mass was predicted using the ProtParam program (27). The molecular masses of the deduced proteins of GhpdxS and GhpdxT were predicted to be 34,104 Da and 23,826 Da, respectively. The expression of rGhpdxS and rGhpdxT represented 55% and 77% in mass of total proteins in the induced crude extract and they were not detectable in an uninduced crude extract **(Fig. 2).**

Approximately 97% of the total rGhpdxS and rGhpdxT expression was in the soluble form. To find an optimal condition to enhance the expression level of rGhpdxS and rGhpdxT, different induction temperatures of 25 °C, 30 °C, and 37 °C, an IPTG concentration up to 1 mM, and different induction times (1,3, and 6 h) were tested. The results showed that the final concentration of 0.2 mM IPTG with an induction time of 3 h at 30 °C was suitable to obtain soluble rGhpdxS and rGhpdxT.

4.2. Purification of Recombinant GhpdxS and GhpdxT

The purification of rGhpdxS was carried out as described in the "Materials and Methods" section of this manuscript. This protocol consisted of three steps as summarized in **Table 2.** The fraction containing rGhpdxS activity was analyzed by SDS-PAGE indicating a single band with a molecular weight of about 35 kDa **(Fig. 3A)**, corresponding to the predicted molecular mass of the monomeric form of the enzyme (34,104 Da). The purification showed that the rGhpdxS was purified 5.8-fold with 71.6% recovery and specific activity of 8.2 $U.mg^{-1}$.

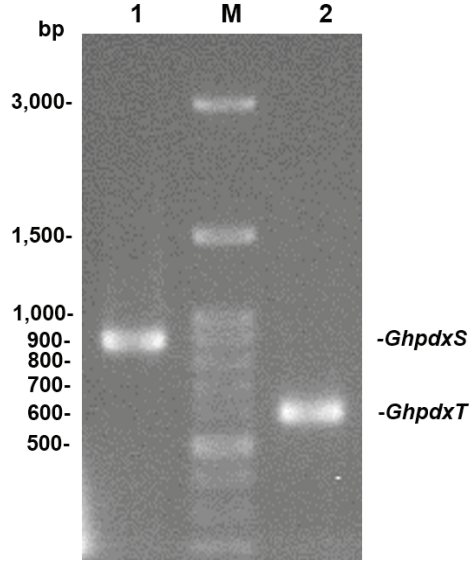

Figure 1. PCR products of *GhpdxS* and *GhpdxT* genes. The product length of the GhpdxS and GhpdxT showed 885 bp and 591 bp, respectively. Lane 1; *GhpdxS* gene, Lane M; 100 bp DNA Ladder (Geneaid), Lane 2; *GhpdxT* gene. The PCR products were analyzed with 1% agarose gel electrophoresis and stained with ethidium bromide.

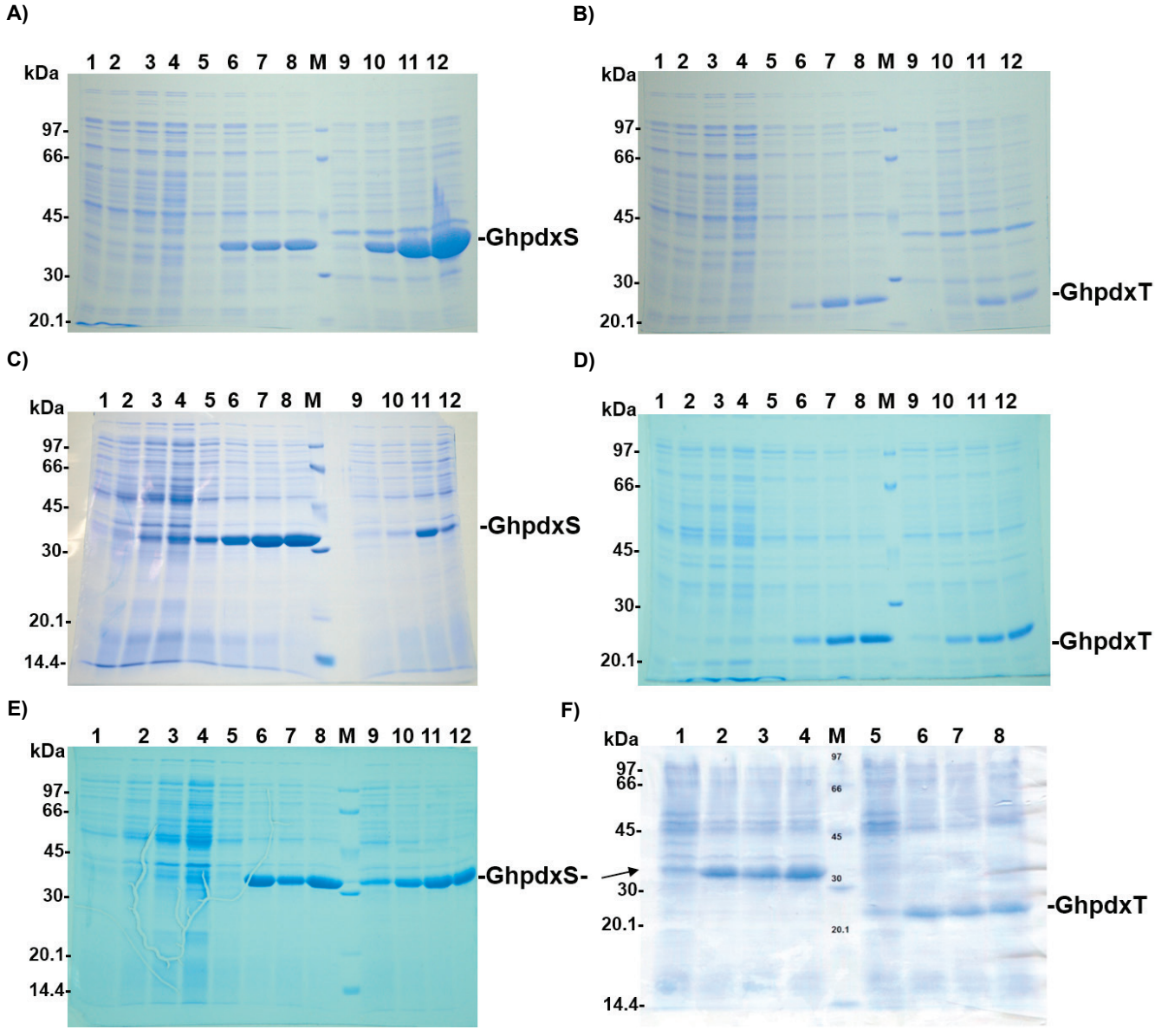

Figure 2. Expression analysis and expression optimization of recombinant GhpdxS and GhpdxT. **(A, C, E)** rGhpdxS expression in 1 mM IPTG at 25, 30, 37 °C, respectively. **B)** rGhpdxT expression in 1 mM IPTG at 25 °C. Lanes 1 to 4: uninduced GhpdxS/T soluble fractions at 0, 1, 3, and 6 h respectively. Lanes 5 to 8: induced GhpdxS/T soluble fractions at 0, 1, 3, and 6 h respectively. Lanes 9 – 12: inclusion body of GhpdxS/T at 0, 1, 3, and 6 h respectively. **D)** rGhpdxT expression in 1 mM IPTG at 30 and 37 °C. Uninduced GhpdxT soluble fractions (Lanes 1 to 4) and induced GhpdxT soluble fractions (Lanes 5 to 8) at 30 °C for 0, 1, 3, and 6 h respectively. Lanes 9 to 12: induced GhpdxT soluble fractions (Lanes 5 to 8) at 37 °C for 0, 1, 3, and 6 h respectively.**F)** expression of rGhpdxS and rGhpdxT at 30 °C by vary IPTG concentration for 6 h. Induced GhpdxS soluble fractions (Lanes 1 to 4) and Induced GhpdxT soluble fractions (Lanes 5 to 8) with 0, 0.2, 0.5 and 1 mM IPTG, respectively. Lane M: protein marker.

Table 2. Purification of rGhpdxS produced by *E. coli* BL21 (DE3).

Purification steps	Total protein (mg)	Total activity (Unit)	Specific activity (Unit/mg)	Purification (fold)	Recovery (%)
Crude extracts	405.90	571.20	1.41	1.00	100.00
Ni Sepharose	158.00	536.00	3.40	2.41	93.84
DEAE cellulose	49.80	409.00	8.21	5.84	71.60

Five grams of cells (wet weight) was used for the purification.

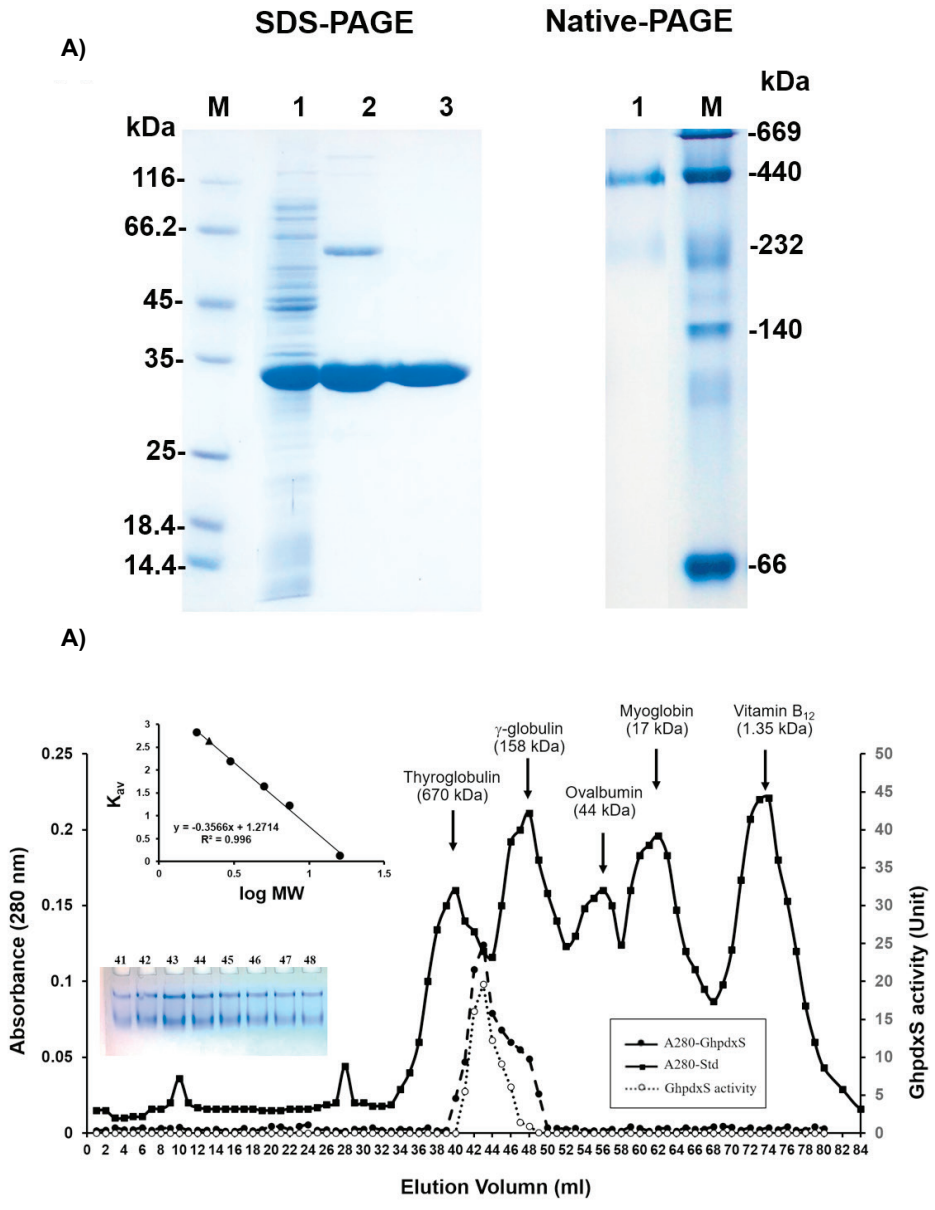

Figure 3. A) SDS-PAGE of rGhpdxS at different steps of purification. Lane M, protein marker; lane 1, crude extracts; lane 2, rGhpdxS purified by Ni-Sepharose 6 Fast Flow column; lane 3, rGhpdxS purified by DEAE-cellulose anion exchange column. 8% Native gel of purified rGhpdxS after DEAE-cellulose anion exchange column. **B)** gel filtration chromatography of rGhpdxS (4 mg, 0.2 mL). Inset, K_{av} of peaks of standard (•) and peak GhpdxS (filled triangle) in logarithmic scale. 8% Native-PAGE of GhpdxS in fraction No. 41- 48 (1 mL/fraction).

The purified rGhpdxS were analyzed on native PAGE. The result showed two different complex formations (hexamer and dodecamer) of rGhpdxS **(Fig. 3A)** with the estimated molecular weights around 210 and 420 kDa, respectively**.** To validate the native molecular weight of the enzyme, the pool fractions containing rGhpdxS eluted from the DEAE cellulose column were run through a Superdex 200 column. A single peak showed in the analytical gel-filtration chromatogram **(Fig. 3B).** The relationship between molecular mass and Ve/Vo shows that the enzyme is about 416 kDa, which corresponds to a dodecameric rGhpdxS.

The purification of rGhpdxT is shown in **Table 3.** After one-step affinity chromatography on Ni Sepharose 6 Fast Flow column, the purified protein showed a single band on the SDS gel **(Fig. 4A)** with 90.97% recovery and specific activity of 18.43 $U.mg^{-1}$. Using a superdex 75 column, the apparent molecular mass of rGhpdxT was estimated to be 23 kDa **(Fig. 4B).** This is similar to the predicted molecular mass of the monomeric form calculated from the amino acid sequence (23,826 Da). The results of native gel and gel filtration confirmed that rGhpdxT was a monomer.

4.3. Biochemical Properties of rGhPLPS

The PdxS and PdxT form PLPS complex to synthesize PLP from G3P, R5P, and glutamine. Using rGhpdxS or rGhpdxT alone could not synthesize PLP from certain substrates. Thus, the two enzymes were mixed in various molar ratios to detect a PLP synthesis activity. The mixture of rGhpdxS and rGhpdxT with a molar ratio of 1:1 showed higher activity than the molar ratio of 1:2 and 1:3 **(Fig. 5A).** Native forms of rGhPLPS and rGhpdxS were compared and shown in **Figure 5B.** The biochemical properties of recombinant PLPS from *Geobacillus* sp. H6a (rGhPLPS) were analyzed by using the ratio of 1:1 of rGhpdxS and rGhpdxT. The effects of pH and temperature were determined using R5P, G3P, and glutamine as substrates. The optimum pH was 9 **(Fig. 6A)**. At pH ranged from 3 to 10, approximately 50% of relative activity was observed when incubated at 25 °C for 60 min. RGhPLPS was likely tolerant to a wide range of pH values. The optimum temperature of rGhPLPS was 70 °C **(Fig. 6B).** The rGhPLPS retained more than 50% of its initial activity after 60 min of incubation at a temperature ranging from 30 to 65 °C, but at 75 and 80 °C, less than 40% of the original activity remained. This result demonstrated that rGhPLPS was a thermophilic enzyme.

The relative activity of rGhPLPS was studied in the presence of various metal ions in concentrations ranging from 0.5 to 10 mM **(Table 4).** The slight activations of rGhPLPS activity were observed in the presence of monovalent cations. All divalent ions decreased enzyme activity when the metal concentration increased except for Mg^{2+}, which slightly promoted enzyme activity at 0.5 mM. The heavy metal ions such as Fe^{2+}, Fe^{3+}, and Cu^{2+} were potent inhibitors of rGhPLPS activity.

The kinetic parameters were determined for the substrates G3P, R5P, and glutamine **(Fig.7).** The *Km* and *Vmax* values of G3P were 195 ± 13.5 µM and 45.1 ± 1.0 $U.mL^{-1}$, respectively. For R5P, *Km* value was 52.3 ± 5.8 µM and *Vmax* was 28.6 ± 0.8 $U.mL^{-1}$, whereas the *Km* and *Vmax* values of glutamine were 5.1 ± 1.1 mM and 32.2 ± 1.1 $U.mL^{-1}$, respectively.

5. Discussion

In order to increase the translational efficiency, the forward primer used for the cloning of *GhpdxS* gene had modified by base substitution from T to A leading to a change in the start codon of *GhpdxS* gene from TTG to ATG, the most common start codon in *E. coli*. More detail had been described by Anutrakunchai *et al* (21).

Table 3. Purification of rGhpdxT produced by *E. coli* BL21 (DE3).

Purification steps	Total protein (mg)	Total activity (Unit)	Specific activity (Unit/mg)	Purification (fold)	Recovery (%)
Crude extracts	13.80	82.47	5.98	1.00	100.00
Ni Sepharose	4.07	75.03	18.43	3.08	90.97

One gram of cells (wet weight) was used for the purification.

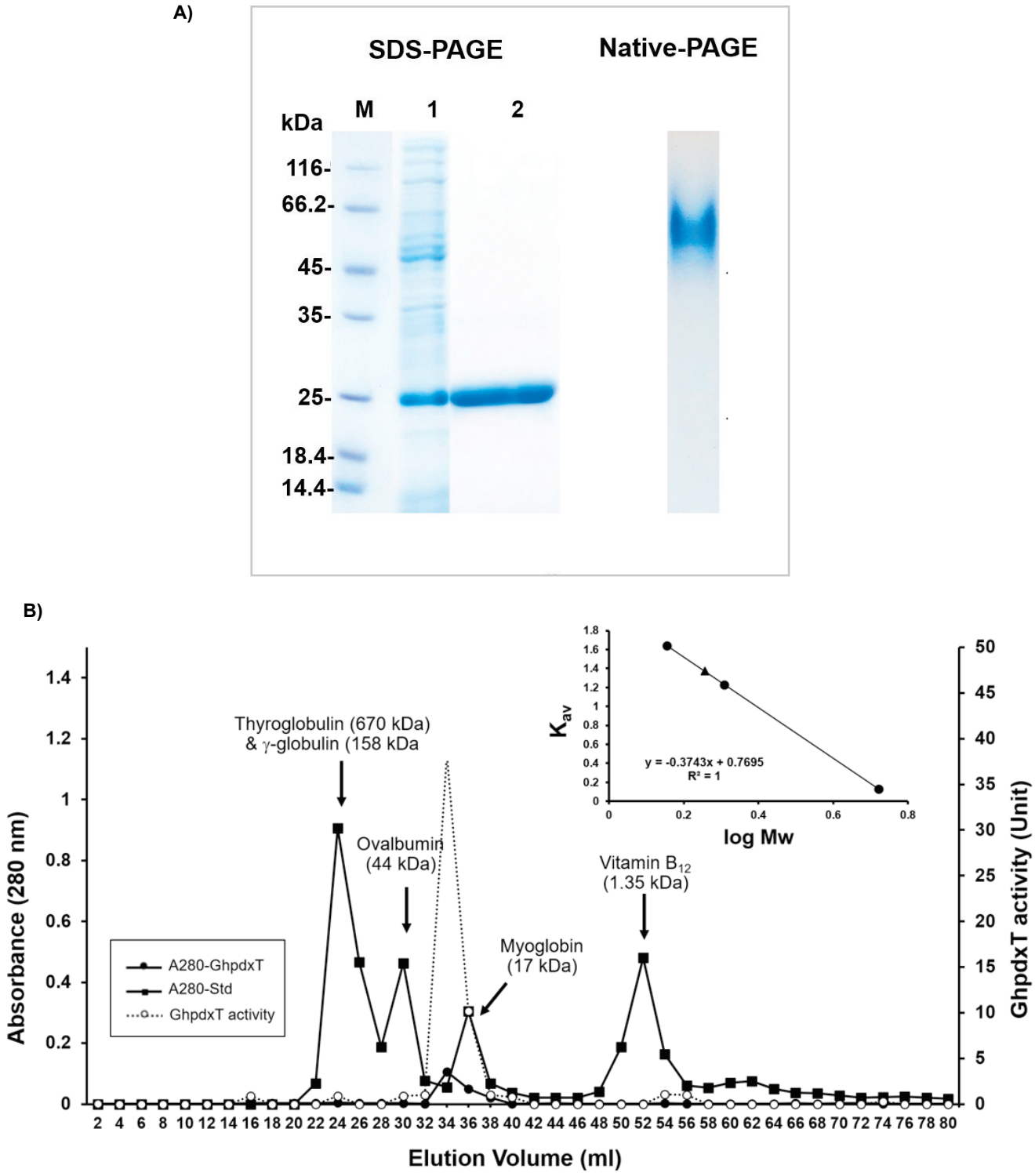

Figure 4. A) SDS-PAGE of rGhpdxT at different steps of purification. Lane M, protein marker; lane 1, crude extracts; lane 2, purified rGhpdxT from Ni Sepharose 6 Fast Flow column. 8% Native gel of purified rGhpdxS. **B)** gel filtration chromatography of rGhpdxT (4 mg, 0.2 mL). Inset, K_{av} of peaks of standard (•) and peak GhpdxS (filled triangle) in logarithmic scale.

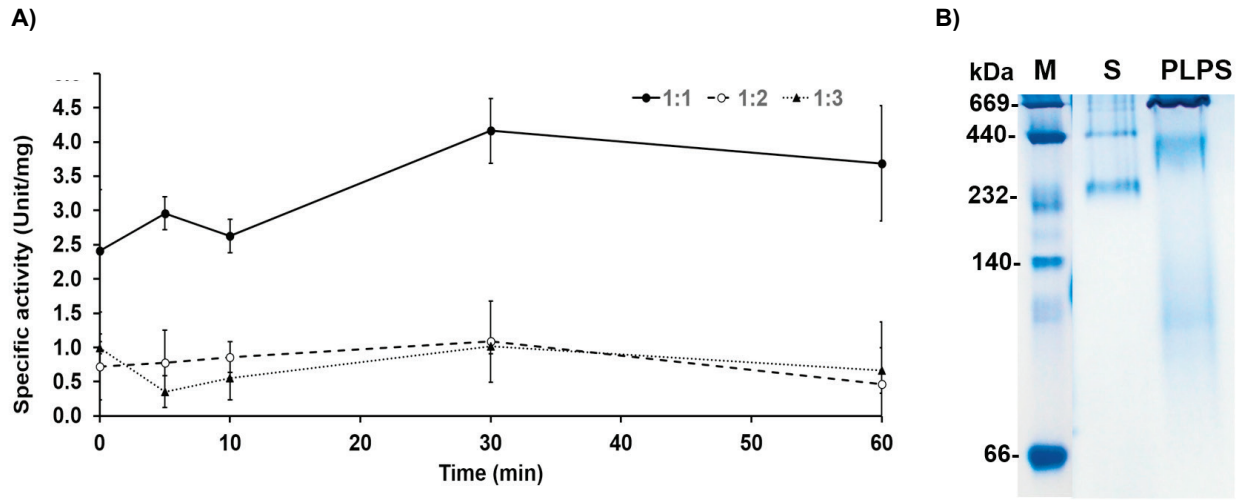

Figure 5. (A) Specific activity of rGhPLPS at different ratio of rGhpdxS and rGhpdxT. Ratio 1:1, 3.67 µM rGhpdxS and 3.67 µM rGhpdxT; ratio 1:2, 3.67 µM rGhpdxS and 7.34 µM rGhpdxT; ratio 1:3, 3.67 µM rGhpdxS and 11.01 µM rGhpdxT. **(B)** 6% Native PAGE. Lane M, protein marker; lane S, purified GhpdxS; lane PLPS, rGhPLPS complex in ratio 1:1.

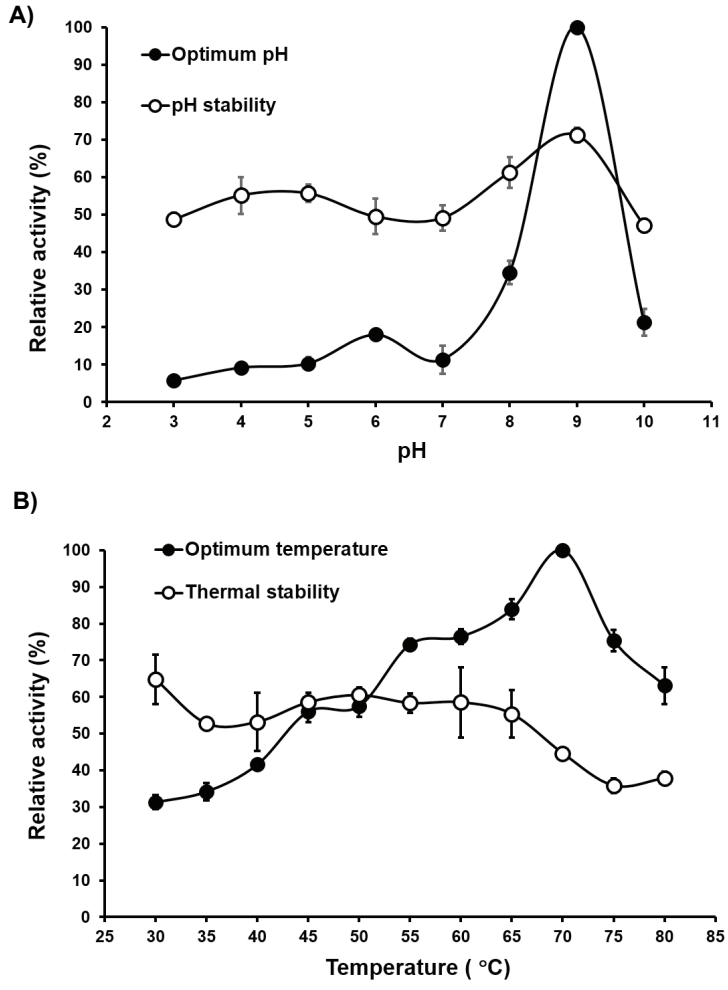

Figure 6. Effects of pH **A)** and temperature **B)** on activity and stability of rGhPLPS.

Table 4. Effects of metal ions on the rGhPLPS activity

Ions	Relative activity (%)		
None	100 ± 1.5		
	0.5 mM	**5 mM**	**10 mM**
K^+	100.3 ± 3.7	103.9 ± 4.3	101.8 ± 3.1
Na^+	106.8 ± 3.9	101.1 ± 1.2	102.3 ± 1.4
Mn^{2+}	83.9 ± 1.2	46.2 ± 4.2	32.7 ± 7.0
Co^{2+}	69.5 ± 8.6	47.9 ± 2.6	35.1 ± 2.0
Cu^{2+}	64.0 ± 2.5	31.2 ± 5.5	26.8 ± 2.2
Ca^{2+}	95.7 ± 8.4	85.9 ± 1.1	84.0 ± 1.2
Ni^{2+}	96.5 ± 1.9	67.6 ± 1.0	61.1 ± 0.9
Mg^{2+}	109.9 ± 5.6	97.1 ± 1.1	89.2 ± 1.0
Zn^{2+}	77.1 ± 8.6	66.0 ± 1.3	50.6 ± 5.6
Fe^{2+}	76.9 ± 1.8	18.4 ± 2.3	8.4 ± 1.7
Fe^{3+}	73.3 ± 1.0	10.0 ± 2.3	4.3 ± 3.5

Note: Relative activity was expressed as a percentage of the mean ± SD.
100% Relative activity was the activity of enzyme in the absence of any metal ions

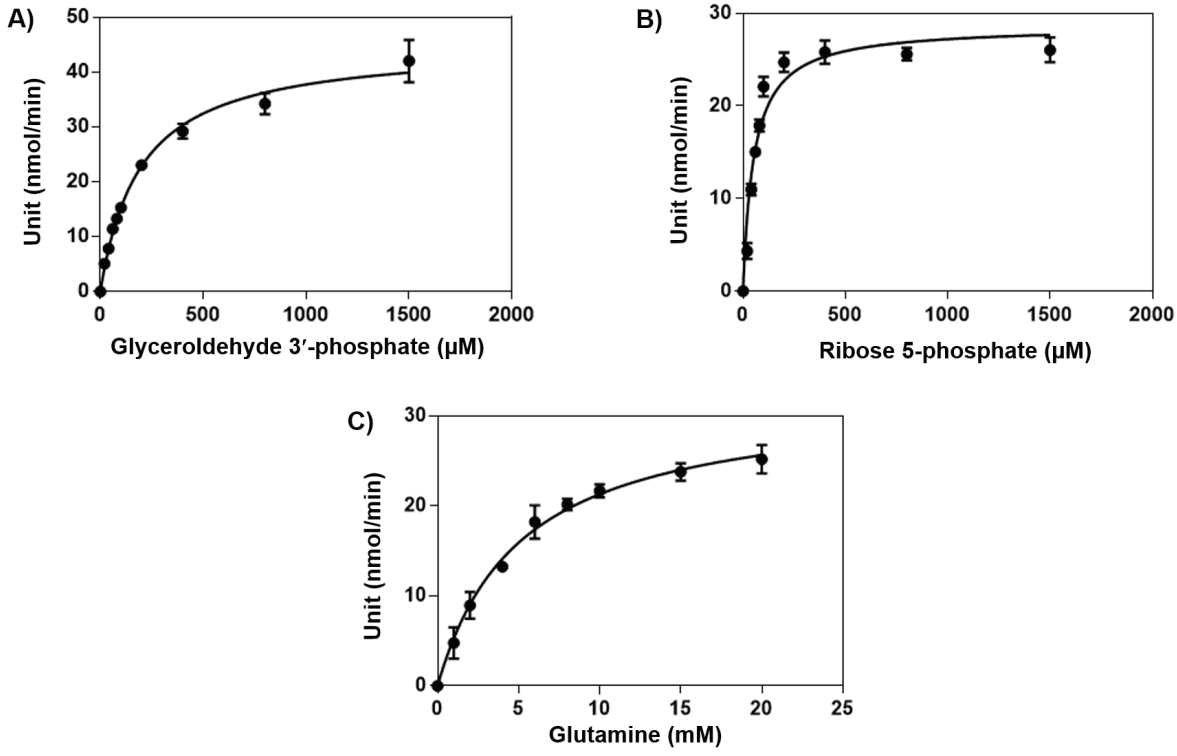

Figure 7. Kinetics of the rGhPLPS reaction. All measurements were done in 50 mM Tris-HCl pH 9.0 at 70°C.

Translation efficiency has been shown to decrease eight-fold when using GTG or TTG as start codons rather than ATG (26).

The native rGhpdxS form **(Fig. 3B)** is almost the same as the other recombinant PdxS enzymes (17, 28, 29). The quaternary structures of *G. stearothermophilus* and *B. subtilis* PdxS determined by ultracentrifugation were studied by Zhu *et al* (28) and Strohmeier *et al* (29), respectively. They reported that PdxS formed hexamer and dodecamer with strong hydrophobic interaction and coexist in a solution, in which the dodecamer is the dominant species (29). To confirm that each form of rGhpdxS is involved in the activity of PLPS, we cut each band in a native gel and examined the activity. The results showed all bands of rGhpdxS could increase absorbance at 405 nm (data not shown).

The structure of PLP synthase from PdxS and PdxT from *G. Sterothermophilus* has been studied (6, 28). The 24-subunit of PLPS comprises 12 PdxS subunits and 12 PdxT subunits. PdxS forms cylindrical dodecamer of two hexameric rings and the active sites are lined on the inner surface of the ring. Each PdxT subunit dock at the outside of the PdxS rings and PdxT active sites point toward the PdxS active sites (28). Native forms of rGhPLPS and rGhpdxS **(Fig. 5B)** are similar to the molecular mass for the 24-subunit as calculated from the 12 rGhpdxS and 12 rGhpdxT subunits (approximately 684 kDa).

rGhPLPS did not require a metal ion for activity; however, some metal ions could alter enzyme activity. Metal ions can participate in enzyme activity in several ways. It can serve as electron donors or acceptors, Lewis acids or structural regulators (30). The earlier report by Raschle *et al*. (23) shown that 1 mM of various metal ions did not affect *B. subtilis* PLPS activities.

We could not explain the difference in metal ion effect between *B. subtilis* PLPS and rGhPLPS activities, since both PdxS and PdxT have different catalytic functions. Further research is needed to analyze the mechanism by which metal ions affect the activity of rGhpdxS, rGhpdxT, or both.

The kinetic parameters yielded values roughly similar to the range reported for *B. subtilis* ($Km = 68 \pm 2$ mM for R5P, 77 ± 2 mM for G3P), *G. sterothermophilus* ($Km = 10 \pm 2$ mM for R5P, 1.06 ± 0.4 mM for G3P) and *S. cerevisiae* ($Km = 3.4$ mM for glutamine) (6, 16).

The rGhPLPS could produce PLP when using G3P and glutamine with Ru5P or R5P as substrates, but PLP could not be produced when using G3P and glutamine with ribose sugar. Furthermore, when DHAP was substituted for G3P in the reaction, PLP could not be detected. This implies that rGhPLPS only can carry out pentose phosphate isomerization and lacks triose phosphate isomerase activity.

To the best of our knowledge, the effects of temperature and pH on PLPS activity have never been reported except one study in *B. subtilis* which exhibited an optimal pH 6 – 6.5 at 37 °C (31). In our study, the effects of temperature and pH on PLPS activity of thermophilic bacterium was the first report. The rGhPLPS was tolerant to wide ranges of temperature and pH values **(Fig. 6).**

Therefore, temperature and pH shift during enzymatic reaction in the industrial process could have a minor influence on its activity. Lacking enantioselectivity of triose phosphate on rGhPLPS may be an advantage in the combination of this enzyme with other enzymes in biocatalytic applications.

6. Conclusions

Cloning, expression, and characterization of recombinant pdxS and pdxT from *Geobacillus* sp. H6a was successfully achieved. The rGhpdxS and rGhpdxT demonstrated activity as synthase and glutaminase, respectively. The highest PLP synthesis activity was received when the mixture of rGhpdxS and rGhpdxT was a molar ratio of 1:1. The rGhPLPS has received considerable interest in the field of biotechnology, as it shows activity in broad ranges of temperatures and pH values. The factors affecting the production of PLP and the means of improving enzyme properties via site-directed mutagenesis should be further studied.

Acknowledgements

The scholarship obtained from Khon Kaen University through National Research University Project (MIH-2554-M-02). This work was granted by Khon Kaen University (No.560014 and No. 570012), Thailand.

References

1. Mooney S, Leuendorf JE, Hendrickson C, Hellmann H. Vitamin B6: A long known compound of surprising complexity. *Molecules*. 2009;**14**(1):329-351. doi: 10.3390/molecules14010329
2. Merigliano C, Mascolo E, Burla R, Saggio I, Verni F. The relationship between vitamin B6, diabetes and cancer. *Front Genet*. 2018;**9**:388. doi: 10.3389/fgene.2018.00388

3. Sangsai A, Moosophon P, Trongpanich Y. Purification of pyridoxamine and pyridoxamine 5′-phosphate from culture broth of *Rhizobium* sp. 6.1C1. *Walailak J Sci Technol*. 2016;**13**:837-847.
4. Ueland PM, McCann A, Midttun Ø, Ulvik A. Inflammation, vitamin B6 and related pathways. *Mol Aspects Med*. 2017;**53**:10-27. doi: 10.1016/j.mam.2016.08.001
5. Commichau FM, Alzinger A, Sande R, Bretzel W, Meyer FM, Chevreux B, *et al*. Overexpression of a non-native deoxyxylulose-dependent vitamin B6 pathway in *Bacillus subtilis* for the production of pyridoxine. *Metab Eng*. 2014;**25**:38-49. doi: 10.1016/j.ymben.2014.06.007
6. Smith AM, Brown WC, Harms E, Smith JL. Crystal structures capture three states in the catalytic cycle of a pyridoxal phosphate (PLP) synthase. *J Biol Chem.* 2015;**290**(9):5226–5239. doi: 10.1074/jbc.m114.626382
7. Zhang X, Teng YB, Liu JP, He YX, Zhou K, Chen Y, *et al*. Structural insights into the catalytic mechanism of the yeast pyridoxal 5-phosphate synthase Snz1. *Biochem J*. 2010;**432**:445-450. doi: 10.1042/bj20101241
8. Gengenbacher M, Fitzpatrick TB, Raschle T, Flicker K, Sinning I, Müller S, *et al*. Vitamin B6 biosynthesis by the malaria parasite *Plasmodium falciparum*: biochemical and structural insights. *J Biol Chem.* 2006;**281**(6):3633–3641. doi: 10.1074/jbc.m508696200
9. Raschle T, Arigoni D, Brunisholz R, Rechsteiner H, Amrhein N, Fitzpatrick TB. Reaction mechanism of pyridoxal 5′-phosphate synthase: detection of an enzyme-bound chromophoric intermediate. *J Biol Chem.* 2007;**282**(9):6098–6105. doi: 10.1074/jbc.m610614200
10. Belitsky BR. Physical and enzymological interaction of *Bacillus subtilis* proteins required for de novo pyridoxal 5′-phosphate biosynthesis. *J Bacteriol.* 2004;**186**(4):1191–1196. doi: 10.1128/jb.186.4.1191–1196.2004
11. Qaidi SE., Yang J, Zhang JR, Metzger DW, Bai G. The vitamin B_6 biosynthesis pathway in *Streptococcus pneumonia* is controlled by pyridoxal 5′-phosphate and the transcription factor PdxR and has an impact on ear infection. *J Bacteriol*. 2013;**195**(10):2187–2196. doi: 10.1128/jb.00041-13
12. Dick T, Manjunatha U, Kappes B, Gengenbacher M. Vitamin B6 biosynthesis is essential for survival and virulence of *Mycobacterium tuberculosis*. *Mol Microbiol*. 2010;**78**(4):980–988. doi: 10.1111/j.1365-2958.2010.07381.x
13. Zein F, Zhang Y, Kang YN, Burns K, Begley TP, Ealick SE. Structural insights into the mechanism of the PLP synthase holoenzyme from *Thermotoga maritima*. *Biochemistry*. 2006;**45**:14609–14620. doi: 10.1021/bi061464y
14. Yoon JY, Park CR, Lee HH, Suh SW. Overexpression, crystallization and preliminary X-ray crystallographic analysis of pyridoxal biosynthesis lyase PdxS from *Pyrococcus horikoshii*. *Acta Cryst*. 2012;**F68**:440–442. doi: 10.1107/s1744309112005829
15. Neuwirth M, Strohmeier M, Windeisen V, Wallner S, Deller S, Rippe K, *et al*. X-ray crystal structure of *Saccharomyces cerevisiae* Pdx1 provides insights into the oligomeric nature of PLP synthases. *FEBS Lett.* 2009; **583**:2179–2186. doi: 10.1016/j.febslet.2009.06.009
16. Dong YX, Sueda S, Nikawa JI, Kondo H. Characterization of the products of the genes *SNO1* and *SNZ1* involved in pyridoxine synthesis in *Saccharomyces cerevisiae*. *Eur J Biochem*. 2004; **271**:745–752. doi: 10.1111/j.1432-1033.2003.03973.x
17. Guédez G, Hipp K, Windeisen V, Derrer B, Gengenbacher M, Böttcher B, *et al*. Assembly of the eukaryotic PLP-synthase complex from *Plasmodium* and activation of the Pdx1 enzyme. *Structure*. 2012;**20**:172–184. doi: 10.1016/j.str.2011.11.015
18. Wrenger C, Eschbach ML, Müller IB, Warnecke D, Walter RD. Analysis of the vitamin B6 biosynthesis pathway in the human malaria parasite *Plasmodium falciparum*. *J Biol Chem.* 2005;**280**(7):5242–5248. doi: 10.1074/jbc.m412475200
19. Leuendorf JE, Genau A, Szewczyk A, Mooney S, Drewke C, Leistner E, *et al*. The Pdx1 family is structurally and functionally conserved between *Arabidopsis thaliana* and *Ginkgo biloba*. *FEBS J*. 2008;**275**:960–969. doi: 10.1111/j.1742-4658.2008.06275.x
20. Anutrakunchai C, Niamsanit S, Wangsomnuk PP, Trongpanich Y. Isolation and characterization of vitamin B_6-producing thermophilic bacterium, *Geobacillus* sp. H6a. *J Gen Appl Microbiol*. 2010;**56**:273–279. doi: 10.2323/jgam.56.273
21. Anutrakunchai C, Niamsanit S, Trongpanich Y. Expression analysis of the Ghpdx1 and Ghpdx2 genes encoding PLP synthase from *Geobacillus* sp. H6a. *KKU Sci J*. 2010;**38**(2):208-220.
22. Bradford MM. A rapid and sensitive method for the quantitation of microgram quantities of protein utilizing the principle of protein-dye binding. *Anal Biochem*. 1976;**72**(1-2):248-254. doi: 10.1016/0003-2697(76)90527-3
23. Raschle T, Amrhein N, Fitzpatrick TB. On the two components of pyridoxal 5′-phosphate synthase from *Bacillus subtilis*. *J Biol Chem.* 2005;**280**(37):32291–32300. doi: 10.1074/jbc.m501356200
24. Wada H, Snell EE. The enzymatic oxidation of pyridoxine and pyridoxamine phosphate. *J Biol Chem.* 1961;**236**(7): 2089–2095. doi:10.1016/s0021-9258(18)64134-1
25. Argoudelis CJ. Simple high-performance liquid chromatographic method for the determination of all seven vitamin B_6-related compounds. *J Chromatogr A*. 1997;**790**(1-2):83-91. doi: 10.1016/s0021-9673(97)00740-1
26. Panicker IS, Browning GF, Markham PF. The effect of an alternate start codon on heterologous expression of a PhoA fusion protein in *Mycoplasma gallisepticum*. *PLoS ONE*. 2015;**10**(5):e0127911. doi: 10.1371/journal.pone.0127911
27. Gasteiger E, Hoogland C, Gattiker A, Duvaud S, Wilkins MR, Appel RD, *et al*. Protein Identification and Analysis Tools on the ExPASy Server. In: Walker JM, editor. The Proteomics Protocols Handbook. New York: Humana Press;2005. p.571-607. doi: 10.1385/1-59259-890-0:571
28. Zhu J, Burgner JW, Harms E, Belitsky BR, Smith JL. A new arrangement of $(\beta/\alpha)_8$ barrels in the synthase subunit of PLP synthase. *J Biol Chem.* 2005;**280**(30):27914-27923. doi: 10.1074/jbc.m503642200
29. Strohmeier M, Raschle T, Mazurkiewicz J, Rippe K, Sinning I, Fitzpatrick TB, *et al*. Structure of a bacterial pyridoxal 5′-phosphate synthase complex. *Proc Natl Acad Sci* USA. 2006; **103**(51):19284-19289. doi: 10.1073/pnas.0604950103
30. Riordan FJ. The role of metals in enzyme activity. *Ann Clin Lab Sci.* 1977;**7**(2):119-129.
31. Burns KE, Xiang Y, Kinsland CL, McLafferty FW, Begley TP. Reconstitution and biochemical characterization of a new pyridoxal-5′-phosphate biosynthetic pathway. *J Am Chem Soc*. 2005;**127**:3682-3683. doi: 10.1021/ja042792t